DAMAGE AND LOSS ASSESSMENT DUE TO TROPICAL CYCLONE IDAI'S FLOODING EVENTS IN CHIMANIMANI DISTRICT

Rumbidzai Chivizhe[1,*], Juliana Useya[1], Reason Mlambo[2] (Zimbabwe)

1. Department of Geomatics Engineering, Faculty of Engineering and Built Environment, University of Zimbabwe, 630 Churchill Avenue, Mt. Pleasant, Harare, Zimbabwe.

2. Department of Surveying and Geomatics, Faculty of Science and Technology, Midlands State University, Private Bag 9055, Senga Road, Gweru, Zimbabwe.

*__Corresponding author:__ rumbidzaisimbo@gmail.com +263774817491

Abstract

The devastating events which befell Chimanimani as a result of Cyclone Idai in March 2019, came with extensive flash flooding, landslides and very high-speed winds which caused huge destruction in the district. Rehabilitation of cyclone affected communities is indispensable to restore livelihoods. The overarching objective of the study is to determine the impacts of Cyclone Idai and conduct damage and loss assessment, focusing on the vegetation, built-up areas and flood extent. This research used Sentinel-1 SAR GRD data to map the flood extent using the pre- and post-flood events images. Then to measure the response of built-up and vegetation to flood events in the Chimanimani district, Sentinel-2 data was used through different indices such as NDVI, NDBI and NDWI which were used in mapping vegetation change and validating flood extents. Images for prior and after the cyclone were used. The results showed that there was a greater negative effect to vegetation due to flooding which occurred mostly along rivers and streams. For the built-up areas affected by floods, the results illustrate that the greater percentage was in the negative change as compared to non-affected built -up areas. This indeed confirms that floods have a negative effect as explained by the houses, bridges and roads that were swept away by water. Cyclone Idai was accompanied by strong winds and flash flooding which both had an effect on the damage and loss that occurred. Therefore, in conclusion, consequential damage and loss due to flash flooding in both vegetation and built-up areas in the Chimanimani district caused a destruction of 93.91% and 28.25% respectively.

KEYWORDS: satellite images, flood mapping, damage and loss assessment

1. Introduction

Natural disasters are calamities with atmospheric, geological, and hydrological causes that have the potential to result in casualties, property destruction, and social and environmental disturbance (Xu et al., 2016). Examples of these natural disasters are, droughts, earthquakes, floods, cyclones and landslides. The most destructive natural disasters are tropical cyclones, which usually pose a significant danger of human fatalities, significant financial loss, and significant environmental damage (Charrua et al., 2021). Some of the tropical cyclones experienced in Zimbabwe included Cyclone Eloise, Tropical Storm Ana, and Cyclone Jasmine, causing significant damage in Zimbabwe (Mukwenha, 2021). In Zimbabwe, the disaster that was experienced in March 2019 was tropical cyclone Idai which was accompanied by flash floods, lightning, hail, and heavy rains. As a result of the catastrophic effects on agriculture, schools, and infrastructure, many residents lost their houses, infrastructural loss, casualties and disruption of daily life (Chatiza, 2019). Fluvial flooding was experienced in Chimanimani district and can be classified into two primary categories: overbank flooding and flash flooding. Flash flooding is defined as a fierce torrent of water over an already-existing river at a fast rate of speed. Flood extent may now be successfully mapped thanks to current technology, such as geographic information systems and remote sensing (Ward et al. 2014; Ho et al. 2010; Samarasinghea et al. 2010).

In this research, the cyclone Idai flood damage and loss assessment was done using both SAR data and optical data; nonetheless, microwave (SAR) satellite data is a more preferable method for flood mapping because it has the ability to capture images day or night regardless of weather conditions (Anusha & Bharathi, 2020). Damage and loss assessment are imperative for flood management although it is a challenging task due to its complexity in dealing with big data, damage types, spatial and temporal scales i.e. depth of analysis (Menoni et al., 2016). GIS and remote sensing, often known as Earth Observation System (EOS), are nowadays the most used tools for disaster management (Simonovic & Eng, 2002). The actual flood extent cannot be assessed fully from field visits because of the area vastness and the restriction of mobility, thus EO data is important (Husain & Shan, 2010). This is because it gives an advantage where data is limited, costly and hard to access and needs frequent revisit times (Clement et al., 2017). Satellite data are crucial for identifying, assessing, and quantifying flood extent, damage, and environmental effects, according to several authors (Hussaina et al. 2011; Khanna et al. 2006). Optical and radar data is common for flood monitoring and damage assessment and proven to be efficient in flood inundation mapping because of their distinct properties. The optical data's distinct water reflectance property makes it effective in identifying water bodies from other land uses as it is displayed in terms of the spectral bands (Husain & Shan, 2010). This property helps to efficiently delineate vegetation from other land covers using a near-infrared and red band optical imagery. Synthetic aperture radar (SAR) sensors' microwave capabilities of being able to penetrate through clouds and its applicability for both day and night makes it extremely good for flood water extraction (Jussi, 2015; Schlaffer et al, 2015). The optical and radar data sets are finally combined through feature level fusion in order to bring out the desired outcome. The radar datasets in this study came from the Sentinel-1 databases, whereas the optical datasets come from Sentinel-2. In this investigation, feature level fusion was used to combine optical and radar data. When two or more images are combined to create a

composite image, the information from each individual image is integrated, giving the finished image a higher information content than any of the input images. "Image fusion" is the name of this procedure (Pradham et al., 2010). Finding a transformation of the original space that would produce these new features, which are conserved or improved to the greatest extent possible, is the aim of feature level fusion.

In terms of Zimbabwe's context, some authors only determined the Cyclone Idai's flood extent while others estimated the general damage and losses that came as a result of the cyclone which did not clearly bring out the exact damage and loss that came as a result of flooding. As a result, the main research gap in the current study is the inadequacy of knowledge regarding the amount of damage and loss that resulted from the cyclone's flood in Zimbabwe's Chimanimani district. Therefore, the objectives of this research are to (i) spatially explicitly map the flooded area extent, (ii)evaluation of the effects of flood brought on by cyclone Idai through moderate spatial resolution imagery (Radar and Optical) and (iii) determining the amount of damage and loss brought on by cyclone Idai's flooding events as per land-use class. The novelty of this study was on using radar in mapping flood extents and then fusing through feature level fusion, with optical data considering spectral indices, thus, NDVI and NDBI. Change detection based on the NDVI and NDBI spectral index on the inundated area is conducted with the intention to determine damage and loss within the study area.

2. Study Area

2.1 Study Area: Chimanimani District

A mountainous district in the Manicaland Province of south-eastern Zimbabwe is the Chimanimani District. The town of Chimanimani also serves as the district capital. It covers an area size of 3,450.14 km2. Its borders are as follows: Mozambique to the east, Mutare District to the north and northwest, Buhera District to the west, and Chipinge District to the south. The eastern portion of the district is bordered by the Chimanimani Mountains, which run for about 50 kilometers (31 miles) and constitute the border with Mozambique. From September 5 to July 20 of each year, Chimanimani experiences 10 months of rain, with a typical 31-day rainfall of at least 0.5 inches. The wettest month is January, with an average rainfall of 7.6 inches, while the driest is August, with an average rainfall of 0.3 inches. Hence, the rainless period of the year lasts for 1.5 months (weatherspark.com). However, rainfall typically consists of powerful thunderstorms and is caused by low pressure systems travelling north-east up the Mozambique channel and inland. Rainfall rises sharply with altitude, reaching 2000mm at higher altitudes from roughly 1200mm annually along south-east-facing foothills (CNR Management Plan, 2010). The majority of the soils in Chimanimani district are white sands, which have a very limited capacity to retain water and low fertility (BirdLife International, 2023).

3. Materials

3.1 Satellite data

3.1.1 Sentinel 1 (SAR/Radar)

For this work, Sentinel-1 Ground Range Detected (GRD) single co-polarized imagery was used to map the flood extent in the study area. It was downloaded from Copernicus Open Access Hub, https://scihub.copernicus.eu/.

3.1.2 Sentinel-2 (Optical)

This study uses Sentinel-2 imagery to evaluate flood damage in the study area. The Copernicus Open Access Hub was used to get the data from the Sentinel-2 SAR satellite operated by the European Space Agency. With spatial resolutions between 10m and 20m, each MSI contains 13 spectral bands that encompass the visible, red-edge, near-infrared (NIR), and short-wave infrared (SWIR) wave lengths. Both the sentinel-1 and sentinel-2 data collected are displayed in Table 1.1 below.

Table 1. Sentinel-1 and Sentinel-2 data acquisition dates

Satellite	Acquisition date before floods	Acquisition date after floods
Sentinel-1	07 March 2019	19 March 2019
Sentinel-2	28 February 2019	25 March 2019

4. Methodology

4.1 Methodology for Radar

The subset of the image, multilooking, radiometric calibration is part of the pre-processing for Sentinel-1's synthetic aperture radar (SAR) data using the Sentinel Snap software. Geometric and radiometric distortion occur as a result of SAR's ability to see the topography from the side. The geometry has been rebuilt using a DEM and is prepared for geometric correction of terrain distortions (Akbari et al., 2012). A digital elevation model (1 Arc Sec SRTM DEM) is used for terrain correction in SAR geocode images to correct for geometric errors and provide a map-projected result. The DEM was downloaded independently for this investigation from USGS Earth Explorer. The data were reprojected using range doppler terrain correction with WGS84. Layer stacking is used to combine the before and after flood images using the VV polarization because it can identify partially submerged features that help assess flood damage (Rao et al., 2006). The

bands from both scenes are combined in the stacked image, therefore in this case, the red band from the before flood and the red and blue bands from the after-flood band were utilized to form the RGB composite. The final image, which was used to produce a flood map as a geotiff which depicts the flood extent. To evaluate the flood damage, the Sentinel-2 NDVI and NDBI scenes will be merged with the flood extent map.

4.2 Methodology for Optical

The Sentinel-2 images that were collected from Copernicus Hub, for this study were on Level 2A and had already undergone radiometric and geometric correction. The atmospheric adjustment was then performed using Sen2Cor by translating the Sentinel-2 Top of Atmospheric Reflectance into the appropriate Bottom of Atmospheric adjusted Level 2A products.

4.2.1 Normalized Difference Vegetation Index (NDVI)

NDVI was employed in this work to track changes in plant cover using the downloaded Sentinel-2 data. An indicator of vegetation greenness used in remote sensing, the Normalized Difference Vegetation Index (NDVI), is linked to the structural characteristics of plants. NDVI time series can be used to analyze the majority of vegetation changes (Forkel et al, 2013). The visible and near infrared portions of the electromagnetic spectrum are used by the NDVI. This is due to the fact that vegetation, such as forests, exhibits substantial absorption in the red area (0.63-0.69u m) and increased reflectance in the near IR range (0.76-0.90u m). The distribution of vegetation is specifically defined by this ratio. The following formula is used to determine NDVI values: NDVI= (NIR-RED/NIR+RED) The NDVI readings are displayed as a ratio from -1 to +1, with the majority of the (-) values denoting water and the rest values falling within the negatives denoting soil/built-up. The categorization considered the variation in NDVI values before and after floods and decided that positive values indicated the presence of vegetation, while negative values indicated that there was no vegetation present and were represented as No Data values.

4.2.2 Normalized Difference Built-up Index (NDBI)

In this study, built-up cover change was tracked using NDBI and the downloaded Sentinel-2 data stated above. The NDBI, which has indices ranging from -1 to 1, is one of the spectral indices designed specifically for extracting man-made surfaces. The electromagnetic spectrum's shortwave-infrared and near-infrared frequencies are used by the NDBI. The following formula is used to determine NDBI values: NDBI= (SWIR-NIR)/(SWIR+NIR). The NDBI values are displayed as a ratio between -1 and +1; the majority of the (-) values correspond to water, while the other numbers within the negatives correspond to vegetation. The categorization considered the variation in NDBI values between before and after floods and decided that positive values indicated the presence of built-up, while negative values indicated the absence of built-up and were represented as No Data values.

4.3 Change detection Statistics for Damage Assessment

All of the photos from before and after the floods in this study were processed using the Change Detection Statistics technique. The flood extent must first be vectorized before the area of interest is clipped in order to construct the subset raster dataset for the flooded-NDVI/NDBI area. NDVI and NDBI were generated for each image as part of the differencing approach, and the resulting images were then used for change detection. This was done to look for changes in the area's built-up areas and vegetation after the floods. The major goal of this exercise was to identify regions that have increased (positive change), decreased (negative change), or remained unchanged. The Differencing Method formulae: NDVI Differencing = NDVInew – NDVIOld and NDBI Differencing = NDBInew – NDBIOld.

4.4 Fusion of Optical and Synthetic Aperture Radar (SAR) data

The generated NDVI and NDBI Difference results were fused using feature level fusion with the vectorized flood extent to extract only the NDVI flooded area and the NDBI flooded area in order to determine both the positive and negative change. The outcome was divided into three categories—decrease, no change, and increase—which clearly demonstrated the amount of the harm. The raster layer unique values report tool was used to collect the statistical values in respect to the decline, no change, and increase class in terms of hectarage.

The flowchart of the methodology in this study area is shown in Figure 2.

Figure 2. Flowchart for the workflow

5. Results and Discussion

5.1 Flood Extent mapping

Sentinel-1 images of the pre- and post-flood events were collected to determine the extent of the flooding episodes under study (Table 1). Water features are distinguished from other features after pre-processing both images using sigma nought (0) distribution as the backscatter coefficient. These backscatter values show the non-water class as higher values and the water class as lower values (Lurist et al., 2017). After thresholding, the research area's water class is generated. After that, the images were combined by building a layer stack with the help of the product's geolocation. The investigation region's water class is generated when the edge is joined. To discriminate between the flooded areas and the permanent water bodies, an RGB composite

image is produced. The pre-flood image fills the red band for this, and the post-flood image fills the blue and green bands.

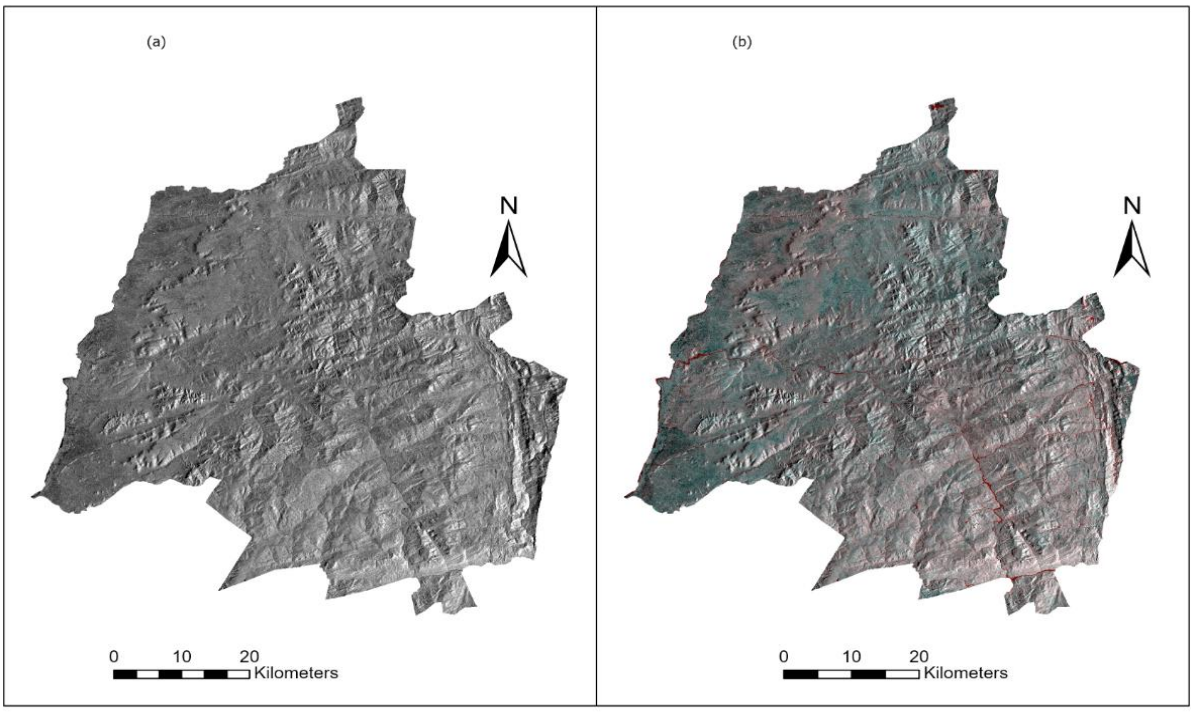

Figure 5. Showing Chimanimani (a) Pre-flood period, with dark gray color representing the river channel and (b) Post-flood period, with the red color representing the flooded river channel.

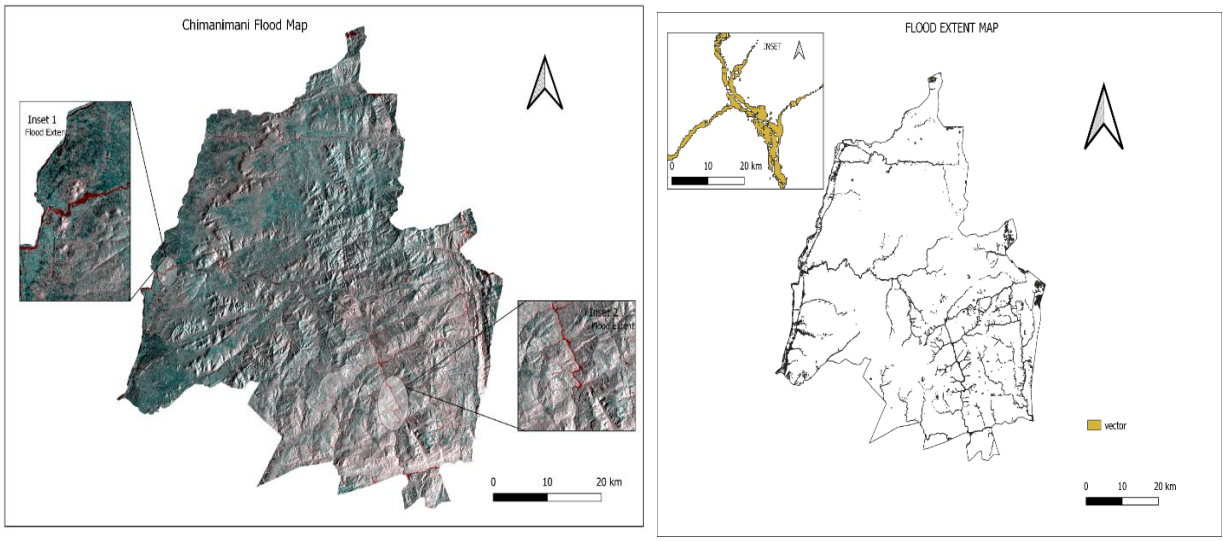

(a) (b)

Figure 6a. Chimanimani area tropical cyclone flood map. Figure 6b. Vectorized flood extent map.

This is done such that the flooded areas on the red channel will have a high radar response because they will land on the pre-flood image, leading to a high backscatter return. However, on the post-flood image, the flooded areas will have a low backscatter return. The purpose of this is to make the flooded areas appear in red because they will have high red channel response and low blue and green channel response, while the surrounding areas where there is no flood appear as tones of grey with a bluish color because they have low backscatter return in both images, which means low response in all the red, green, and blue bands. To determine the extent of flooding caused by the cyclone, water features of the flooding were mapped, and the results were compared with permanent water bodies. The flooded area in comparison to non-flooded area is shown on Figure 5 whilst the Chimanimani flood map is clearly depicted in Figure 6a. The flooded areas are then vectorized by exporting the map of the affected area as a geotiff; the vector map is depicted in figure 6b.

The red tones symbolize flood surfaces where the water has totally flooded, while the light pink tones are typical of humid environments. The distinction of flooded areas is best when the polarization is chosen correctly (Klemas, 2015). The findings from our polarization configurations and the contributions from studies comparing polarizations to monitor flood zones confirm that the VV polarization is more effective at delimiting flooded areas (Martinis & Rieke, 2015). It creates well-defined surfaces with the ability to identify partially submerged features, providing data that VH polarization may not be able to provide because it is predicated on the terrain's heterogeneity and roughness (Manjusree et al., 2012).

The validation of the flood extent was carried out by extracting the extent of the flood using NDWI, which produced results that were identical, particularly with regard to the flooding in rivers and permanent water bodies. The same SAR method was tested in order to map the flood extent in Mozambique, and it was successful in doing so.

5.2.1 Impacts of flood on Vegetation using NDVI

NDVI values range from -1 to +1, the non-vegetation class is eliminated from the analysis by reclassifying before and after flood images. Figure 8 shows the NDVI before and after flood map. On the basis of the classified image, NDVI Difference is then determined and the results of the change detection are presented on Figure 9. The five classes used to depict the NDVI Differencing results above are more increase, less increase, no change, less decline, and more decrease. Although the flooded areas exhibit the complete opposite, the data indicate that there are often more locations with vegetation that has somewhat increased than those shown by the "less increase" class. The places with a greater loss of vegetation, in particular, are depicted as having vegetation inside of flooded areas. The sentinel-1 resultant vectorized image showing the flood extent is merged with the Sentinel-2 NDVI change image. This gives us the flooded area NDVI change layer as shown in Figure 10 below.

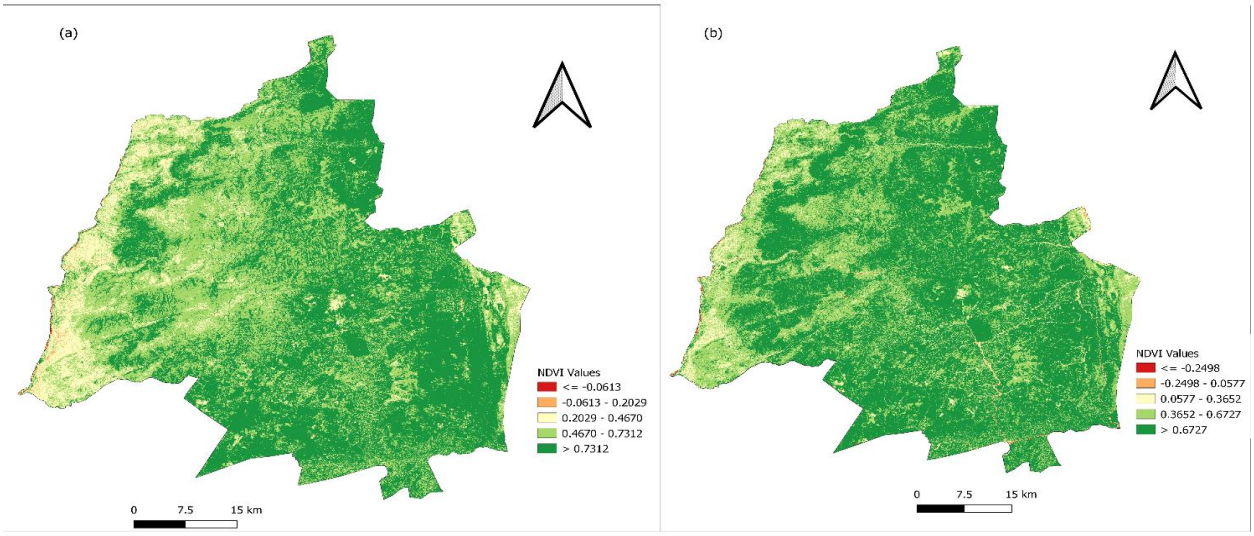

Figure 8. Showing (a) NDVI Pre-flood period and (b) NDVI Post flood period.

The change detection statistics are calculated based on the extracted flooded NDVI change area with reference to the changes represented in the figure above. The more decrease and less decrease are classified as negative change, the less increase and more increase as positive change while no change remains the same. The results are shown in Table 2.

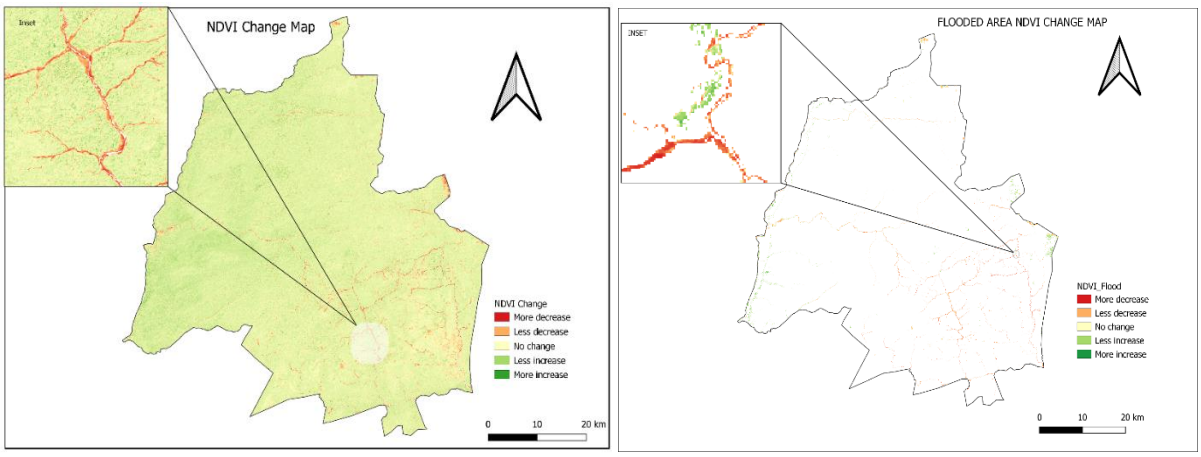

(a) (b)

Figure 9 (a) Shows the NDVI Change Detection for cyclone Idai flooding event and Figure 9 (b). showing the flooded area NDVI change scenes.

Table 2. Change detection statistics for vegetation

Class	Area	% Change
Positive change	236.57 Ha	5.98
No change	4.33 Ha	0.11
Negative change	3716 Ha	93.91

According to the table, the class of depleted vegetation is exhibiting the highest change, with a change of 93.91 percent, compared to vegetation that saw no change as a result of flooding, with a change of 0.11 percent. The 5.98 percent margin represents the vegetation that changed more than average. The estimation of the damage and loss experienced in terms of vegetation is 93.91% which corresponds to 3716Ha of negative change. This means then that almost all the vegetation that was mainly along the river beds was damaged by the flash floods experienced during cyclone Idai among other flooded areas. The no change and positive change representing no damage, corresponds to some vegetation that adapts to flood such as a number of tress like acacia and mopane and some rice plants which flourish with too much water present.

5.2.2 Impacts of flood on built-up areas using NDBI

There was a need to exclude the non-built up areas from the differencing process, hence any feature which corresponded to non-built up was assigned no data value. The image that results is utilized to determine the NDBI Difference. Figure 8 below shows the results of the change detection calculations for the Cyclone Idai flood occurrences.

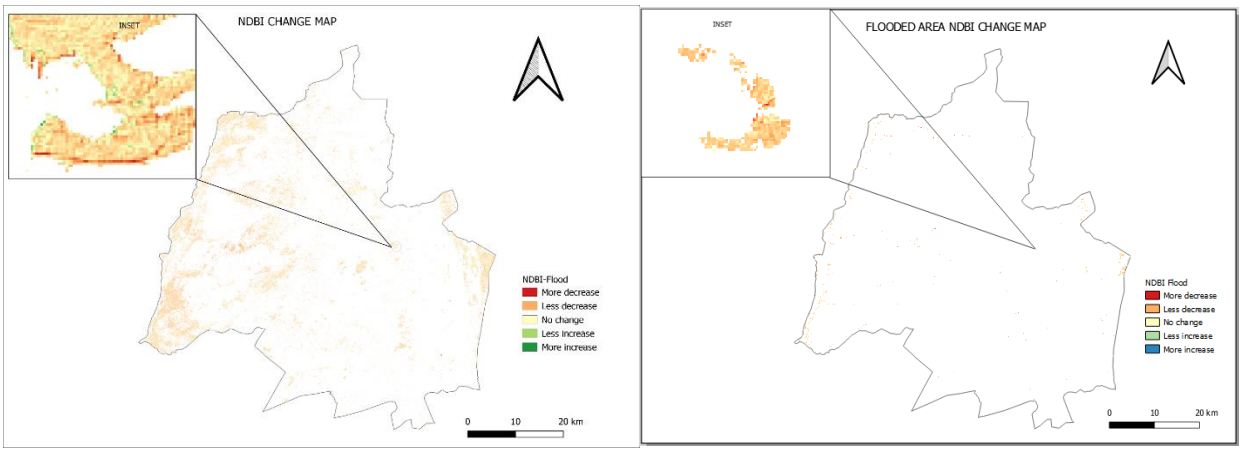

(a) (b)

Figure 12a. Showing NDBI change and Figure 12b. Showing the flooded area NDBI change scenes

The figure 12a above shows the NDBI change for periods between before and after flood. The results indicate that, there has been a significant decline in built-up, no change regions and a less pronounced increase in built up areas. The sentinel-1 resultant vectorized image showing the flood extent is merged with the sentinel-2 NDBI change image. This gives us the flooded area NDBI change layer as shown in Figure 12b. The following table was created with reference to changes that have taken place since the cyclone Idai flood event using the change detection statistics in QGIS. The no change class stays the same while the more decrease and less decrease classes are combined to form the negative change class and the more increase and less increase classes are combined to form the positive change class. The findings of the change detection are shown in Table 3 below in three groups for positive change, no change, and negative change.

Table 3. Change detection statistics for built-up areas

Class	Area	% Change
Positive change	233.60 Ha	20.56
No change	581.58 Ha	51.19
Negative change	320.98 Ha	28.25

The findings from this study, demonstrate that indeed floods have an effect on built-up areas. The positive change in built-up areas, of hectarage as 233.60Ha, giving us an estimate of 20.56 percent. This damage presented by 28.25 percent is explained by the houses, bridges and roads that were swept away by water. No change which has a highest representation of 51.19 percent, shows us that vast areas which were made up of infrastructure were not affected by flood, hence the structures are still intact. The positive change however, could mean those buildings that were immediately erected after flood for resettlement and also a few drawbacks of using NDBI such as noise due to some barren ground particularly uncultivated arable land which may have similar spectral response patterns. According to the Government of Zimbabwe data by Chatiza (2019), 61.5% of dwellings in Chimanimani were damaged. Since a variety of elements, such as landslides, wind, stones falling, and water, contributed to the damage to homes in Chimanimani. We therefore conclude that 28.25% of the 61.5 % of damaged dwellings in Chimanimani were caused by flood.

6. Analysis of Results

The storm left a path of destruction causing the deaths of people as well as significant damage to crops, livestock, and property. Road infrastructure was grossly damaged with above 90% of road networks in Chimanimani and Chipinge damaged and 584 km of roads being damaged by

landslides. Bridges were also swept away. The shortage of fit for human habitation land has forced some people to settle along waterways that are prone to landslides and there is also apparent stream bank farming around many rivers and river sources (Munsaka et al, 2021). The building materials commonly used for construction of walls and roof of houses in rural areas are clay, sand, bamboo, grass, reeds, timber and stone. These can be easily washed away by floods especially if built along waterways. On the other hand, bridges and roads which also fall under the category of built-up areas were constructed using steel, concrete, stone and asphalt, had several of them washed away by the flood due to the pressure caused by the flood. There is also an issue of degraded land observed in soil compaction, increased run-off, loss of soil fertility, and decrease in vegetation cover which cause low river volumes thus increasing the vulnerability to flooding and landslides (Munsaka et al, 2021). According to assessment by the Environmental Management Agency (EMA) in 2009, areas affected by water were mainly located in floodplains, along waterways and on steep slopes. This was evident as presented on the flood map on figure 6 which shows that flood was mostly along the river course. Extreme seasonal changes in monthly rainfall occur in Chimanimani, which accounts for cyclone Idai's appearance in March 2019 as one of the anomalies. People in Chimanimani district have most of their planting and irrigation close to the rivers, these are plants such as bananas, yam, maize and some tea estates were negatively damaged by the floods. There was also a case of insects which came as a result of the flood that destroyed a certain maize field. According to my research, of the total area of Chimanimani district which is 3,450.15km2, about 5882.32Ha was submerged under water during cyclone.

7. Conclusion

The study's main objective was to evaluate the damage and loss which came as a result of flooding in Chimanimani district due to tropical cyclone Idai in March 2019. This was achieved by using Sentinel-1 SAR data to map the flood extent and Sentinel-2 data to determine the vegetation and built-up affected by flood. For analysis, this was later combined through feature level fusion to determine the damage and loss on the flooded areas only. A lot of vegetation was affected by cyclone Idai compared to the infrastructure that was destroyed by the cyclone. The rehabilitation efforts, as explained before, should target first those inhabitants along waterways and on floodplains as they were the most affected by floods. Particularly vulnerable to flooding were the Ngangu, Kopa, and other residential areas, which were exposed more than other regions (Munsaka et al, 2021). A key factor in lessening a community's vulnerability to disasters is the town planners and local institutions' ability to do their duties. The capacity of communities to prepare for and respond to flooding is increased by climate risks education and awareness. This research is unique in that it has distinguished between the loss and damage brought on by Cyclone Idai's flooding events compared to those that considered it in general. There were however, limitations due to the image's resolution which made it difficult to assess damage per each vegetation type and built-up class in particular which I would recommend the other researchers to further the study by focusing on the specifics given higher resolution imagery.

References

Akbari, V., Larsen, Y., Doulgeris, A. P., & Eltoft, T., 2012. The impact of terrain correction of polarimetric SAR data on glacier change detection. In International Geoscience and Remote Sensing Symposium (IGRASS), pp. 5129-5132.
Anusha, N., & Bharathi. V., 2019, Flood detection and flood mapping using multi-temporal synthetic aperture radar and optical data. The Egyptian Journal of Remote Sensing and Space Science. 23.
Arun, R. & Premalatha, K., 2020. Flood Damage Assessment Using Remote Sensing and GIS: The Past and Present. International Journal of Civil Engineering and Technology (IJCIET), 11(12), pp. 1-15.
BirdLife International, 2023, BirdLife International's Position on Climate Change. Cambridge, Uk.
Charrua, A. B., 2021, Impacts of the Tropical Cyclone Idai in Mozambique: A Multi-Temporal Landsat Satellite Imagery Analysis. Remote Sensing, 13(201).
Chatiza, K., 2019. Cyclone Idai in Zimbabwe. An analysis of policy implications for post-disaster ins disaster risk management, p. 2.
Clement, M. A., Kilsby, C. G. & Moore, P., 2017, Multi-temporal synthetic aperture radar flood mapping using change detection. Journal of Flood Risk Management, pp. 0-17.
CNR Management Plan, 2010, Agro Ecological Regions and Climate of Chimanimani, Appendix2
Forkel, M., Carvalhais, N., Verbesselt, J., Mahecha, M. D., Neigh, C. S., & Reichstein, M., 2013, Trend change detection in NDVI time series: Effects of inter-annual variability and methodology. Remote Sensing. 5(5), 2113-2144.
Hussaina, E., Urala, S., Malikb, A. & Shana, J., 2011, Mapping Pakistan 2010 floods using remote sensing data: ASPRS Annual Conference. Milwaukee, WI, USA, s.n.
Hussain, E. & Shan, J., 2010, Mapping major floods with optical and sar satellite images. IEEE Geoscience and Remote Sensing Symposium, Honolulu, Hawaii, USA, (July), pp. 25-30.
International Federation of Red Cross and Red Crescent Societies, 2019, Zimbabwe: Tropical Cyclone Idai, s.1: International Federation of Red Cross and Red Crescent Societies
Jussi, M., 2015, Synthetic Aperture Radar based flood mapping in the Alam-Pedja Nature Reserve in years 2005-2011.
Klemas, V., 2015, Remote sensing of floods and flood-prone areas. An Overview. J. Coast. Res. 31, pp. 1005-1013.
Lurist, N., Lurist, N.V., Oniga, V.E., Statescu, F. and Marcu, C., 2012, Floods damage estimation using Sentinel-1 satellite images. Case study-GALATI COUNTY, ROMANIA.
Martinis, S. & Rieke, C., 2015, Backscatter analysis using multi-temporal and multi-frequency SAR data in the context of flood mapping at river Saale, Germany. Remote Sensing, 7, pp. 7732-7752.
Menoni, S., Molinari, D., Ballio, F., Minucci, G., Mejri, O., Atun, F., Berni, N., and Pandolfo, C., 2016, Flood damage: a model for consistent, complete and multipurpose scenarios, Nat. Hazards Earth Syst. Sci., 16, 2783–2797

Mukwenha S, 2021. Health emergency and disaster risk management: A case of Zimbabwe's preparedness and response to cyclones and storms: We are not there yet, Harare: Public Health in Practice.
Munsaka, E., Mudavanhu, C., Sakala, L., Manjeru, P., Matsvange, D., 2021, When Disaster Risk Management Systems Fail: The Case of Cyclone Idai in Chimanimani District, Zimbabwe. International Journal of Disaster Risk Science, 12, pp. 689-699.
Pradhan, B.,2010, Flood susceptible mapping and risk area delineation using logistic regression, GIS and remote sensing. J Spatial Hydrol 9:1–18
Rao, G. S., Brinda, V., Sree, P. M., & Bhanumurthy, V. 2006, Advantage of Multi-polarized SAR data for Flood Extent Delineation. 64100.
Schlaffer, S., Matgen, P., Hollaus, M. & Wagner, W., 2015, Flood detection from multi-temporal SAR data using harmonic analysis and change detection. International Journal of Applied Earth Observation and Geoinformation, Volume 38, pp. 15-24.
Simonovic, S. P. & Eng, P., 2002, Role of remote sensing in disaster management, s.l.: s.n.
Ward, D. et al., 2014. Floodplain inundation and vegetation dynamics in the Alligator rivers region (kakadu) of northern Australia assessed using optical and Radar Remote Sensing. Remote Sensing of Environment,147, pp. 43-55. https://doi.org/10.1016/j.rse.2014.02.009
Xu, J., Wang Zi., Shen, F., Ouyang, C., Tu, Y., 2016, Natural disasters and social conflict: A systematic literature review, International Journal of Disaster Risk Reduction,17, pp. 38-48.

BIOGRAPHICAL NOTES (Corresponding author)

Rumbidzai Chivizhe

2012-2017 Bsc Honors Degree Surveying and Geomatics (Midlands State University)

2017-2022 Land Surveyor in Training (D. Chigumbu Land Surveyors- Zimbabwe)

2021-2023 Honorary Treasurer (Survey Institute of Zimbabwe)

2021-2022 Msc Geomatics Engineering (University of Zimbabwe)

CONTACTS

Mrs Rumbidzai Chivizhe

Survey Institute of Zimbabwe, Suite4, Phyllis Court, 3 Raleigh Street, Harare, Zimbabwe

Email: rumbidzaisimbo@gmail.com